IN-PLANE BEHAVIOUR OF TUFF MASONRY STRENGTHENED WITH INORGANIC MATRIX-GRID COMPOSITES IN DIAGONAL COMPRESSION

F. Parisi, I. Iovinella*, A. Balsamo, N. Augenti, A. Prota

Dept. of Structural Engineering, University of Naples Federico II, via Claudio 21, 80125 Naples, Italy
**ivano.iovinella@unina.it*

Keywords: tuff masonry, inorganic matrix-grid composites, external strengthening, diagonal compression tests.

Abstract

Tuff masonry structures are a large part of the existing cultural heritage in Mediterranean countries and need to be preserved against earthquakes by reversible strengthening systems. External strengthening with mortar-based composites can give a crucial contribution to this challenge because higher bond to masonry substrates is ensured and further disadvantages of resin-based composites are reduced. In this paper, diagonal compression tests on tuff masonry specimens before and after the application of an inorganic matrix-grid (IMG) composite are discussed. Three IMG layouts were investigated: single-side strengthening; single-side strengthening with steel fibre-reinforced polymer (SFRP) ties; and double-side strengthening. A gradual increase in shear strength was observed from single- to double-side strengthened specimens. Single-side strengthening without SFRP ties caused lower ductility.

1 Introduction

Lateral strength of individual masonry walls plays a crucial role in seismic design and assessment of masonry constructions based on global analysis of simplified macro-element capacity models. Although masonry is typically an assemblage of bricks/stones and mortar joints, it is assumed to be an equivalent homogenous material with elastic-plastic behaviour in compression and zero/limited tensile strength within macro-element models [1]. A masonry wall can fail in shear sliding, diagonal tension cracking, or flexure, depending on its material properties, height/length ratio, applied axial force and boundary conditions [2]. Shear sliding can develop along a single mortar bed joint or both bed and head joints in a stepwise way. Diagonal tension cracking consists in the formation of a single diagonal crack which typically involves both mortar joints and masonry units. Finally, flexural failure consists of masonry crushing at compressed wall corners which can be preceded by tensile cracking at opposite corners of end sections. Tensile cracking induces rigid-body (rocking) rotations of the masonry wall. The failure mode can change from as-built to strengthened conditions. Many masonry structures are located in earthquake-prone regions and need to be retrofitted. In this context, interesting applications involve the use of composite materials which do not cause significant increase in both inertia mass and lateral stiffness, opposed to some traditional strengthening systems (e.g., reinforced plaster, post-tensioning, grout injections). The effectiveness of fibre-reinforced polymers (FRPs), used in the form of both laminates and near-surface mounted bars, has been assessed in a number of studies [3–5] and analytical

capacity models have been provided by recent guidelines to predict the contribution of FRPs to lateral strength of masonry walls [6,7]. Nevertheless, resin-based composites have the following disadvantages: sensitivity to high temperatures, moisture impermeability, flammability, and poor bond to existing masonry substrates. Such problems can be overcome by mortar-based composites which ensure satisfactory bond also to high-porosity masonry substrates. Past experimental programs [8,9] have assessed innovative strengthening systems based on cementitious mortar matrices, highlighting significant improvements in both in-plane and out-of-plane lateral strength of masonry walls. Given that such systems are continuous over the masonry wall, premature failure due to debonding does not typically occur. These considerations motivated the authors to investigate the in-plane behaviour of tuff masonry walls externally strengthened with an inorganic matrix-grid (IMG) composite, which has already been applied on a full scale masonry wall with opening subjected to in-plane lateral loading test [10]. Tuff masonry is typically composed by tuff stones and lime or pozzolana-based mortar joints, with or without inner core; its high porosity make mortar matrices very attractive for retrofitting. In addition, tuff masonry structures are widely spread in Mediterranean countries and often belong to the cultural heritage, so they are to be preserved in accordance with worldwide principles of reversibility and minimum intervention.

2 Experimental program

Past laboratory tests were carried out to characterise tuff stones, mortar, and also tuff masonry as a whole [11]. Then, mechanical properties of IMG system matrix and grid were derived by laboratory tests and supplier's reports, respectively, in order to complete mechanical characterisation of constituent materials. The experimental program presented in this study consisted in diagonal compression tests on both as-built and strengthened tuff masonry specimens. Such "indirect" tests were preferred over "direct" shear-compression tests because of their limited cost and duration for setup preparation, both laboratory and on-site performability, and ability to provide valuable estimates of mechanical properties used in analytical models [12]. Actually, the diagonal compression test is the standard method in some national and international codes such as FEMA 356 [13] and the Italian Building Code Commentary (IBCC) [14], especially in the case of existing masonry assemblages. Two different interpretations of diagonal compression test are provided by ASTM E 519-07 [15] and RILEM TC 76-LUM [16].

2.1 Description of specimens

Tuff masonry specimens with running bond and two leaves were tested and were 310×1230×1230 mm in size. Tuff masonry was made of tuff stones with dimensions 100×150×300 mm and pozzolana-based mortar joints of thickness 10 mm. Diagonal compression tests were carried out on 3 as-built specimens and 6 strengthened specimens with the following layouts: (1) single-side strengthening; (2) single-side strengthening with steel fibre-reinforced polymer (SFRP) ties; and (3) double-side strengthening. The IMG strengthening system was made of a special two-component inorganic matrix and a GFRP coated grid (Fig. 1a), and was realised as follows: masonry pre-wetting and first coating with 6 mm thick matrix layer; hand-pressing of GFRP grid into the wet binder with fibres aligned to mortar joints of tuff masonry; and second coating with 6 mm thick matrix layer (Fig. 1b). The nominal thickness of the IMG strengthening system was then 12 mm. The construction procedure of IMG strengthening system with SFRP ties was approximately the same (Fig. 2). Five 250 mm deep holes were realised in the specimen prior to the application of the first matrix layer. Then, SFRP ties of length 500 mm, which were previously impregnated with epoxy resin, were inserted in the holes in a way to spread one half of their length within square pockets over the grid. Finally, square pockets were filled with mortar.

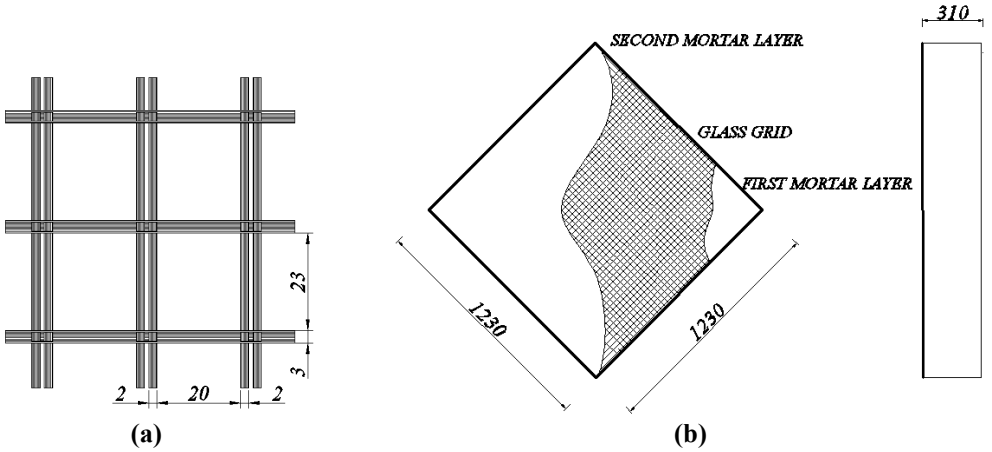

Figure 1. (a) Grid geometry; (b) IMG strengthening system (dimensions in mm).

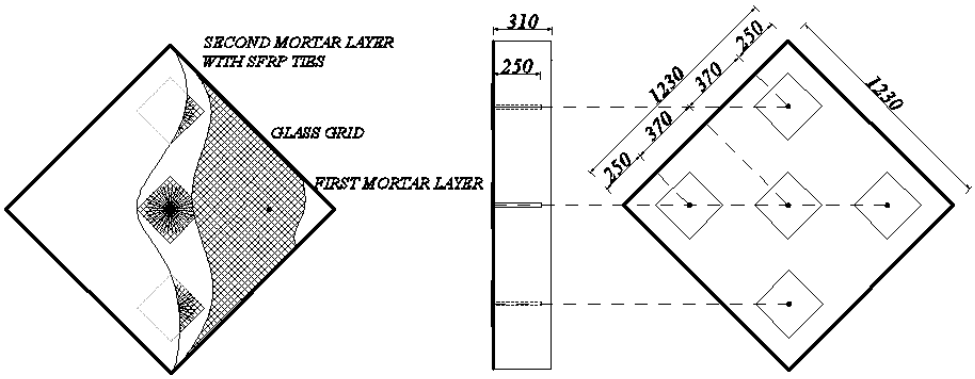

Figure 2. IMG strengthening system with SFRP ties (dimensions in mm).

2.2 Material properties

Tuff stones had a unit weight of 11.72 kN/m^3. Uniaxial compressive tests on 6 cubic tuff specimens with edge 70 mm were carried out in accordance with EN1926 [17] (Table 1). Tensile strength was derived by direct tensile testing on tuff specimen with dimensions 100×100×200 mm and notch in mid section, according to Almeida et al. [18]. Young's and shear moduli were estimated on 6 tuff specimens 70×70×140 mm in size, according to EN14580 [19]. A premixed hydraulic mortar with mean unit weight 16.92 kN/m^3 was used for tuff masonry joints; it was composed by natural sand with 1:6.25 water/sand ratio by weight and pozzolana-like reactive aggregates. Laboratory tests on mortar specimens were carried out in accordance with European standards [20,21]. Compressive tests on 6 cubic mortar specimens with edge 40 mm. That mortar is classified as M2.5 by Eurocode 6 [22] and Italian Building Code (IBC) [23]. Young's and shear moduli were estimated on 3 specimens with dimensions 70×70×140 mm. Finally, tensile strength of mortar was characterised on 3 specimens which were 40×40×160 mm in size. The IMG system matrix was made of hydraulic lime and sand (ratio by weight 1:3) added with glass fibres (ratio by total weight 1:10) and mixed with latex and water (ratio by weight 2:1).

Material	f_c **[MPa]**	f_t **[MPa]**	E **[GPa]**	G **[GPa]**
Tuff stones	4.13	0.23	1.54	0.44
Pozzolana-based mortar	2.50	1.43	1.52	0.66
IMG system matrix	16.05	6.00	8.00	–
IMG system grid	–	1276	72.0	–

Table 1. Mechanical properties of constituent materials.

The glass fibre-reinforced matrix ensured higher ductility and tensile strength, resulting in a high-performance composite. The grid was a bidirectional alkali-resistant glass coated net with approximately 25 mm spacing, 225 g/m^2 unit weight, and 1.77% ultimate strain. The inorganic matrix was characterised through laboratory tests on 8 specimens with dimensions 40×40×160 mm, which were cured for 28 days at standard moisture and temperature levels [20,21]. Mechanical properties of GFRP grid were provided by its supplier.

2.3 Test setup, instrumentation and procedure

Diagonal compression tests were carried out through universal testing machine Italsigma. Diagonal compression was applied by an hydraulic actuator through steel shoes which were fixed at opposite specimen corners to avoid local crushing of masonry (Fig. 3). Diagonal compression was then applied in displacement control at a rate of 15 μm/s until approximately 25% of peak force was reached on the post-peak softening branch of the force–displacement diagram. Relative displacements along specimen diagonals were measured on each side by linear variable differential transformers (LVDTs) with gage length 400 mm.

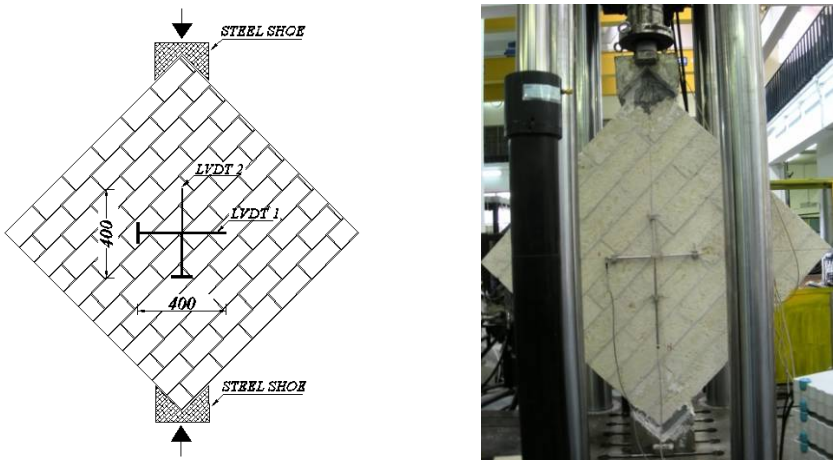

Figure 3. Test setup.

3 Crack patterns

As-built specimens suffered stair-stepped cracking involving both bed and head joints along their compressed diagonal (Figs. 4a–c). Tensile cracking of some tuff stones was detected on P2 specimen (Fig. 4b), resulting in higher strength and lower ductility especially compared to P1 specimen (see Sect. 4). In fact, bed joint sliding typically produces higher dissipation. Figures 5a–c (single-side strengthened specimen) and 6a–c (single-side strengthened specimen with SFRP ties) show small cracks on the IMG system side, large cracks on the masonry side, and out-of-plane bending with elongation at the masonry side. Such a bending was probably caused by cracking onset on the masonry side (as a result of significantly lower tensile strength of masonry compared to that of the IMG system) and its propagation towards the IMG system side of specimens. This unfavourable mechanism occurred after peak load was reached, causing significant strength degradation as fracture process propagated from the masonry to the IMG system side. Crack propagation also produced a progressive reduction in the effective masonry cross section, that is, the compressed portion of initial cross section. Large cracks with a width up to 52 mm were detected also in the case of single-side strengthened specimens with SFRP ties. Nevertheless, out-of-plane bending was less significant especially in the case of PRF1 specimen. The IMG strengthening system suffered larger cracks which essentially followed stair-stepped failure of inner tuff masonry during diagonal compression tests on double-side strengthened specimens (Figs. 7a–b). On the other hand, no out-of-plane deformations were observed on them (Fig. 7c).

(a) **(b)** **(c)**

Figure 4. Crack patterns of as-built specimens: (a) P1; (b) P2; (c) P3.

(a) **(b)** **(c)**

Figure 5. Crack patterns of PR1 specimen: (a) IMG system side; (b) Masonry side; (c) Lateral view.

(a) **(b)** **(c)**

Figure 6. Crack patterns of PRF2 specimen: (a) IMG system side; (b) Masonry side; (c) Lateral view.

(a) **(b)** **(c)**

Figure 7. Crack patterns of double-side strengthened specimens: (a) PRR1; (b) PRR2; (c) Lateral view.

4 Analysis of experimental results

Force and displacement readings of diagonal compression tests were processed according to RILEM TC 76-LUM [15] and ASTM E 519-07 [16], which are based on different interpretation models. The former is based on the solution for a homogeneous, elastic isotropic shell subjected to in-plane diagonal compression. Shear stress is not assumed to be uniform along the height and Mohr's circle is not centred. Conversely, a shear stress state at zero confining stress is assumed by ASTM E 519-07 at the centroid of specimen, resulting in a shear stress equal to both tensile and compressive principal stresses. Diagonal cracking is then assumed to be caused by the attainment of masonry tensile strength f_t, which is equal to shear strength at zero confining stress τ_0. This equality does not apply in the test interpretation by RILEM TC 76-LUM where shear stress at any diagonal compressive load P and shear stress at zero confining stress are approximately 48 and 24% higher than those provided by ASTM E 519-07, while a 31% lower tensile strength is obtained. Based on displacement readings on both specimen sides, axial strains along a single direction were derived as average displacement readings divided by the gage length. Horizontal and vertical strains of the same side were then summed up at each compressive load level to get the corresponding shear strain. Figures 8a and 8b show shear stress versus shear strain diagrams according to RILEM TC 76-LUM and ASTM E 519-07, respectively. Relevant parameters are outlined in Tables 2 and 3 where: ν is the Poisson's ratio; G is the shear modulus; τ_u is the ultimate shear stress at 0.8 times the first-peak shear stress τ_{max}; γ_{max} is the shear strain at τ_{max}; γ_u is the ultimate shear strain at τ_u; and μ is the shear strain ductility defined as $\mu = \gamma_u/\gamma_{max}$.

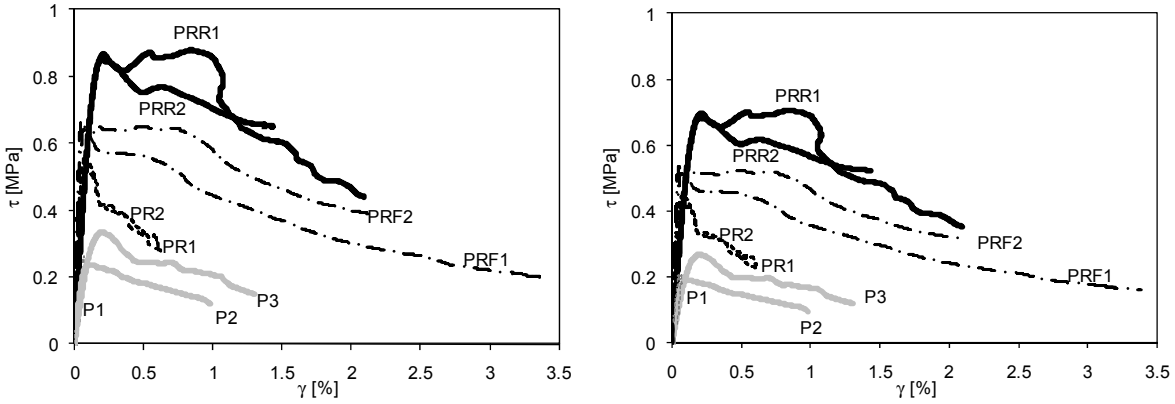

Figure 8. Shear stress versus shear strain diagrams: (a) RILEM TC 76-LUM; (b) ASTM E 519-07.

Both diagrams and tables demonstrate a gradual increase in shear strength from single- to double-side strengthened specimens where the presence of SFRP ties produced not only an intermediate shear strength, but also a significant improvement in terms of ductility.

Specimen	τ_0 [MPa]	f_t [MPa]	ν [–]	G [MPa]	τ_u [MPa]	γ_{max} [%]	γ_u [%]	μ [–]
P1	0.24	0.13	0.35	439	0.19	0.11	0.41	3.6
P2	0.34	0.19	0.32	289	0.27	0.20	0.37	1.9
P3	0.26	0.12	0.47	793	0.21	0.05	0.06	1.4
PR1	0.56	0.26	0.62	1417	0.45	0.08	0.17	2.2
PR2	0.51	0.24	0.79	1757	0.40	0.10	0.31	3.1
PRF1	0.67	0.31	1.00	2370	0.53	0.05	0.68	13.8
PRF2	0.65	0.30	0.77	1846	0.52	0.18	1.18	6.7
PRR1	0.88	0.49	0.37	702	0.70	0.21	1.09	5.2
PRR2	0.85	0.47	0.44	718	0.68	0.20	1.12	5.5

Table 2. Mechanical properties estimated in accordance with RILEM TC 76-LUM.

Nonetheless, single-side strengthened specimens were apparently stiffer due to different axial strain readings on specimen sides. Whilst mean ductility reduced from as-built to single-side strengthened specimens, it was 3.9 times higher in the presence of SFRP ties. Tables 2 and 3 confirm that shear and tensile strength predictions complying with RILEM TC 76-LUM [15] are respectively higher and lower than those according to ASTM E 519-07 [16].

Specimen	τ_0 [MPa]	f_t [MPa]	ν [–]	G [MPa]	τ_u [MPa]	γ_{max} [%]	γ_u [%]	μ [–]
P1	0.19	0.19	0.35	352	0.15	0.11	0.41	3.6
P2	0.27	0.27	0.32	232	0.22	0.20	0.37	1.9
P3	0.21	0.21	0.47	637	0.17	0.05	0.06	1.4
PR1	0.45	0.45	0.62	1138	0.36	0.08	0.17	2.2
PR2	0.41	0.41	0.79	1412	0.32	0.10	0.31	3.1
PRF1	0.53	0.53	1.00	1904	0.43	0.05	0.68	13.8
PRF2	0.52	0.52	0.77	1483	0.42	0.18	1.18	6.7
PRR1	0.71	0.71	0.37	564	0.57	0.21	1.09	5.2
PRR2	0.68	0.68	0.44	577	0.55	0.20	1.12	5.5

Table 3. Mechanical properties estimated in accordance with ASTM E 519-07.

5 Conclusions

An experimental investigation aimed at assessing the effectiveness of the IMG strengthening system to improve shear behaviour of tuff masonry has been presented. Tuff masonry specimens were tested in both as-built and strengthened conditions under in-plane diagonal compression. The following IMG layouts were considered: single-side strengthening; single-side strengthening with SFRP ties; and double-side strengthening. As-built specimens suffered stair-stepped cracking; single-side strengthened specimens with and without passing-through SFRP ties experienced small cracks on the IMG system side and large cracks on the masonry side, which were associated with out-of-plane bending. In the absence of SFRP ties, that bending produced lower ductility compared to other strengthened specimens even though shear strength was higher than that of as-built specimens. The inclusion of SFRP ties in single-side strengthened specimens increased both shear strength and ductility. Double-side IMG strengthening allowed further improvement in shear behaviour, eliminating out-of-plane bending in the post-peak softening phase. Experimental results were processed in separate ways on the basis of RILEM and ASTM standards. Mean shear strength and ductility of as-built specimens were in agreement with past tests, while significantly lower strength values are suggested by IBCC. Shear strength increase factors equal to 1.9, 2.4 and 3.1 were estimated in the case of single-side strengthened specimens, single-side strengthened specimens with SFRP ties and double-side strengthened specimens, respectively. Ductility increase factors equal to 1.1, 4.5 and 2.3 were also derived for the aforementioned specimens. On the other hand, past tests on CMG strengthened specimens [8] showed a mean increase in shear strength and ductility equal to 2 and 1.4, respectively. The effectiveness of IMG strengthened system is then higher with the exception of single-side layout without SFRP ties, which provides about the same shear strength increase but only a 10% increase in ductility. It is also underlined that traditional strengthening based on double-side reinforced plaster with and without transverse steel ties is expected to provide lower shear strength increase factors of 2 and 1.33, respectively, according to IBCC. In addition, the IMG strengthening system is approximately 10 mm thick on each side, while reinforced plaster has typically thickness of 100–200 mm resulting in significant mass increase, and hence more severe seismic actions on the masonry structure.

Acknowledgements

This research was carried out in the framework of the ReLUIS-DPC 2010–2013 project (Line

AT1–1.1 – 'Evaluation of the Vulnerability of Masonry Buildings, Historical Centres and Cultural Heritage') funded by the Italian Department of Civil Protection. MAPEI spa is also gratefully acknowledged for providing strengthening materials.

References

[1] Augenti N. *Il calcolo sismico degli edifici in muratura*. UTET, Turin, Italy (2000), in Italian.
[2] Magenes G., Calvi G.M. In-plane seismic response of brick masonry walls. *Earthquake Engineering and Structural Dynamics*, **26**, pp. 1091-1112 (1997).
[3] Valluzzi M.R., Tinazzi D., Modena C. Shear behaviour of masonry panels strengthened by FRP laminates. *Construction and Building Materials*, **16**, pp. 409-416 (2002).
[4] Marcari G., Manfredi G., Prota A., Pecce M. In-plane shear performance of masonry panels strengthened with FRP. *Composites Part B*, **38**, pp. 887-901 (2007).
[5] Marcari G., Oliveira D.V., Fabbrocino G., Lourenço P.B. Shear capacity assessment of tuff panels strengthened with FRP diagonal layout. *Composites: Part B*, **42**, pp. 1956-1965 (2011).
[6] CNR-DT 200. *Guide for the design and construction of externally bonded FRP systems for strengthening existing structures* (2004).
[7] ACI440.7R-10. *Guide for the design and construction of externally bonded fiber-reinforced polymer systems for strengthening unreinforced masonry structures* (2010).
[8] Prota A., Marcari G., Fabbrocino G., Manfredi G., Aldea C. Experimental in-plane behavior of tuff masonry strengthened with cementitious matrix-grid composites. *Journal of Composites for Construction*, **10**, pp. 223-233 (2006).
[9] Papanicolau C.G., Triantafillou T.C., Papathanasiou M., Karlos K. Textile reinforced mortar (TRM) versus FRP as strengthening material of URM walls: Out-of-plane cyclic loading. *Materials and Structures*, **41**, pp. 143-157 (2008).
[10] Augenti N., Parisi F., Prota A., Manfredi G. In-plane lateral response of a full-scale masonry sub-assemblage with and without an inorganic matrix-grid strengthening system. *Journal of Composites for Construction*, **15**, pp. 578-590 (2011).
[11] Augenti N., Parisi F. Constitutive models for tuff masonry under uniaxial compression. *Journal of Materials in Civil Engineering*, **22**, pp. 1102-1111 (2010).
[12] Turnšek V., Čačovič F. *Some experimental results on the strength of brick masonry walls* in "Proceedings of 2nd International Brick and Block Masonry Conference", Stoke-on-Trent, UK (1970).
[13] FEMA 356. *Prestandard and commentary for the seismic rehabilitation of buildings* (2000).
[14] Circolare 02.02.2009, n. 617. *Istruzioni per l'applicazione delle «Nuove Norme Tecniche per le Costruzioni» di cui al decreto ministeriale 14 gennaio 2008* (2009), in Italian.
[15] RILEM TC 76-LUM. *Diagonal tensile strength tests of small wall specimens* (1994).
[16] ASTM E 519-07. *Standard test method for diagonal tension (shear) in masonry assemblages* (2007).
[17] EN1926. *Natural stone test methods – Determination of compressive strength* (1999).
[18] Almeida J.C., Lourenço P.B., Barros J.A. *Characterization of brick and brick-mortar interface under uniaxial tension* in "Proceedings of 7th International Seminar on Structural Masonry for Developing Countries", Belo Horizonte, Brazil (2002).
[19] EN14580. *Natural stone test methods – Determination of static elastic modulus* (2005).
[20] EN1015-11. *Methods of test for mortar for masonry – Part 11: Determination of flexural and compressive strength of hardened mortar* (1999).
[21] EN998-2. *Specification for mortar for masonry – Masonry mortar* (2003).
[22] EN1996-1-1. *Eurocode 6: Design of masonry structures – Part 1-1: General rules for reinforced and unreinforced masonry structures* (2005).
[23] D.M. 14.01.2008. *Norme Tecniche per le Costruzioni* (2008), in Italian.